MAGNETIC RESONANCE IN MEDICINE 3, 15–23 (1986)

# Real-Value Representation in Inversion–Recovery NMR Imaging by Use of a Phase-Correction Method

H. W. PARK, M. H. CHO, AND Z. H. CHO*

*Department of Electrical Science, Korea Advanced Institute of Science, P.O. Box 150, Cheongryangni, Seoul, Korea*

Received January 11, 1985; revised April 25, 1985

A new technique of real-value representation in inversion–recovery (IR) imaging by use of a phase-correction method is proposed. In this scheme, negative magnetizations at the beginning of the inversion point ($T_I \simeq 0$) are correctly represented as negative values rather than positive. By use of this new scheme, a consistent IR image set as a function of several inversion times ($T_I$) can be obtained. The latter, i.e., consistent image set which represents the real value of $T_1$ weighted images at several inversion times is important in the search for tumors and abnormalities since the inversion time ($T_I$) in the pulse sequence strongly affects $T_1$ contrast. 

## INTRODUCTION

Among the NMR imaging pulse sequences (*1–6*) most often used the inversion–recovery (IR) imaging sequence is least used for a number of reasons. First, the imaging time of IR imaging is usually longer than the time needed in the saturation–recovery (SR) imaging, and second, images obtained at different inversion times ($T_I$) appear with contrast reversal at certain inversion times $T_I$, e.g., at short times $T_I$ (*7–11*). This contrast reversal is the result of the fact that conventional IR imaging usually takes the magnitude of the signal thereby eliminating the polarity information of the signal (*7, 9, 11*). This phenomenon has sometimes caused confusion in image interpretation. More recently, tumor and other abnomalities can be identified using a SR pulse sequence with a combination that uses a long echo time $T_E$ as well as long repetition time $T_R$, i.e., as long as 100 ms and 2.0 s or more, respectively, to enhance $T_2$ dependency of image contrast (*7, 9*). Due to these increasing trends of imaging time, interest in IR imaging seems to be reviving and new approaches for the improvement of the IR imaging are being sought (*7–11*). Among these approaches, in a method according to Bakker *et al.* the signal polarity has been recovered by using a set of inversion–recovery NMR images obtained with several different inversion times (*10*).

In this paper, a simple phase-correction scheme with which it is possible to accurately estimate the phase and polarity is proposed. The consistent results of this scheme in clinical trials indicate the usefulness of the method in tumor identification. With this technique, no abrupt contrast reversal is observed over the entire range of inversion time ($T_I$), therefore, the results are much more consistent for tumor indications. In

* Also at the Dept. of Radiological Sciences, University of California, Irvine, California, 92717.



0740-3194/86 $3.00

the following, the theory associated with the phase correction in IR imaging and subsequent experimental verification of the proposed method will be given.

## THE THEORY OF INVERSION–RECOVERY (IR) IMAGING (7–11)

Conventional SR imaging is employed to generate $T_1$-dependent spin-density images. Inversion–recovery (IR) imaging is believed to enhance further $T_1$ dependency of image contrast compared to SR and SE (spin-echo) imagings, usually by a factor of two in image contrast affected by $T_1$. Let us briefly review the conventional IR pulse sequence which often uses spin echoes for convenience (see Fig. 1) (8).

In this sequence, at first, 180° inversion rf pulse (the first rf) is followed by a 90° rf pulse (the second rf) with inversion time interval $T_I$. Usually both 180 and 90° rf pulses are slice-selective pulses in conjunction with $z$ gradient $G_z$ ($z$ axis is a selecting direction) for a single slice imaging. A spin echo produced by an additional 180° selective rf pulse (the third rf) is usually used for practical convenience. $y$ gradient $G_y$ is used for phase encoding while $x$ gradient $G_x$ is being applied for the FID or echo signal readout. Analytically, the echo signal (sometimes noted as FID) which is obtained with the above described pulse sequence (see Fig. 1) can be written as

$$S_I(t_x, t_y) = \int\int dx dy \rho_I(x, y) \exp(i\gamma x G_x t_x + i\gamma y G_y t_y) \qquad [1]$$

where

$$\rho_I(x, y) = \rho(x, y) \exp\left(-\frac{T_E + t_x}{T_2}\right) \qquad [2]$$

$$\times \left\{1 - 2\exp\left(-\frac{T_I}{T_1}\right) + 2\exp\left(-\frac{T_R - T_E/2}{T_1}\right) - \exp\left(-\frac{T_R}{T_1}\right)\right\}$$

and $\rho(x, y)$ is 2-D spin-density function, $\gamma$ is gyromagnetic ratio, and symbols given by $T_R$, $T_I$, $T_E$, $G_x$, $G_y$, $t_x$, and $t_y$ are the parameters given in Fig. 1. For simplicity, let us eliminate the $T_2$-dependent term $\exp(-(T_E + t_x)/T_2)$ in Eqs. [1] and [2]. In Fig. 1 and real experiment, varying amplitude ($g_y$) and fixed pulse duration ($T_y$) are used for the $y$ gradient. But variable $t_y$ and fixed value $G_y$ are used instead of $T_y$ and $g_y$, respectively, for mathematical convenience in these equations. By taking the Fourier transform of the echo signal $S_I(t_x, t_y)$, a $T_1$-dependent spin-density image function $f_I(\omega_x, \omega_y)$ can be obtained, i.e.,

$$f_I(\omega_x, \omega_y) = \mathcal{F}_2[S_I(t_x, t_y); \quad t_x \rightarrow \omega_x, t_y \rightarrow \omega_y] \qquad [3]$$

where $\omega_x = \gamma G_x x$, $\omega_y = \gamma G_y y$, and $\mathcal{F}_2[\cdot]$ is the 2-D Fourier transform operator. As can easily be shown from Eq. [2], the polarity of the signal is dependent on the inversion time $T_I$ and spin–lattice relaxation time $T_1$. When an object consists of regions having different $T_1$ values but with same spin densities, the region with shorter $T_1$ should have larger values than regions with larger $T_1$ values. This contrast should be consistent throughout the inversion time $T_I$, although contrast ratio could vary with different $T_1$ values.

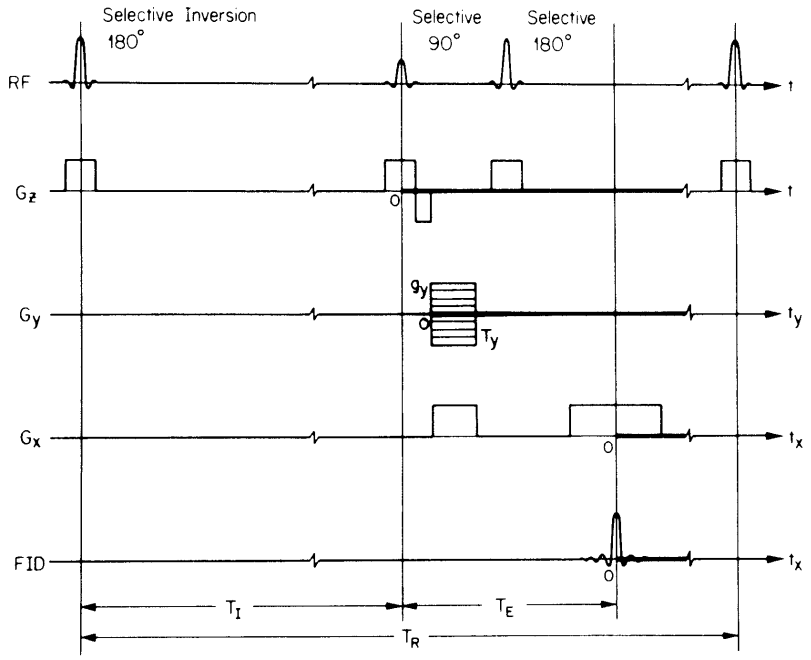


FIG. 1. Pulse sequence for the conventional inversion-recovery imaging using the magnitude method.

For tumor imaging, due to the unknown nature of various tumor spin–lattice relaxation times $T_1$, IR imagings with several different $T_I$ values are usually necessary and information on the nature of tumor and abnormalities can be deduced from those sets of data. Interpretation of IR images will be extremely confusing and even destructive if image contrasts are changed abruptly at a certain inversion time $T_I$. It will be most desirable to show an image set whose contrasts vary continuously as a function of inversion time $T_I$. As has been mentioned, however, the image contrasts are reversed at short $T_I$ values since echo signals obtained by a conventional IR technique are processed by a magnitude method such as the following.

*Magnitude Technique and Contrast Reversal at Short $T_I$ Values (12, 13)*

Let the experimentally obtained echo signal by the pulse sequence shown in Fig. 1 be given by

$$\tilde{S}_I(t_x, t_y) = S_I(t_x - \beta, t_y)\exp(i\alpha) \qquad [4]$$

where $\beta$ and $\alpha$ are the phase-shift terms. $\beta$ mainly results from rise and fall times of gradient pulses, effect of eddy currents on gradient pulses, and frequency-dependent phase delay of electronic circuits. $\alpha$ is the constant phase shift resulting from the phase delay of electronic circuits such as low-pass and bandpass filters and other electronic channels.

To obtain $T_I$ weighted spin-density image $f_I(\omega_x, \omega_y)$ from the experimentally obtained echo signal of Eq. [4], a 2-D Fourier transform of $\tilde{S}_I(t_x, t_y)$ is taken as follows:

$$\tilde{f}_I(\omega_x, \omega_y) = \int\int dt_x dt_y \tilde{S}_I(t_x, t_y)\exp\{-i(\omega_x t_x + \omega_y t_y)\}$$

$$= \int\int dt_x dt_y S_I(t_x - \beta, t_y)\exp(i\alpha)\exp\{-i(\omega_x t_x + \omega_y t_y)\}. \quad [5]$$

The reconstructed $\tilde{f}_I(\omega_x, \omega_y)$ of Eq. [5] can be represented with ideal $T_1$ weighted spin density $f_I(\omega_x, \omega_y)$ with phase-shift terms, i.e.,

$$\tilde{f}_I(\omega_x, \omega_y) = f_I(\omega_x, \omega_y)\exp\{i(\alpha - \beta\omega_x)\}. \quad [6]$$

Therefore, $T_1$ weighted spin density $f_I(\omega_x, \omega_y)$ which is given by Eq. [3] can theoretically be reconstructed from $\tilde{f}_I(\omega_x, \omega_y)$ obtained from Eq. [5], if the phase-shift terms ($\beta$ and $\alpha$) are known. In conventional IR imaging, however, the magnitude technique is used to obtain $T_1$ weighted spin-density images, i.e., by simply taking the magnitude of Eq. [6]. $T_1$ weighted spin density $f_I(\omega_x, \omega_y)$ can then be obtained as a magnitude form, i.e.,

$$|\tilde{f}_I(\omega_x, \omega_y)| = |f_I(\omega_x, \omega_y)|. \quad [7]$$

Although Eq. [7] eliminates the phase-dependent terms by taking magnitude, this technique results in polarity reversal for the negative values of spins at short $T_1$ values, since the terms in the $|\tilde{f}_I(\omega_x, \omega_y)|$ always become positive. The images obtained by this technique, therefore, can be misinterpreted, especially when echo signals (or FID signals) are obtained at short inversion time $T_1$. Results of this effect are illustrated in Fig. 2 where two exponential lines indicate the recovery process of two materials having different relaxation times. The effect of this contrast reversal obtained experimentally with a human brain often results in misinterpretation of the images as will be shown latter.

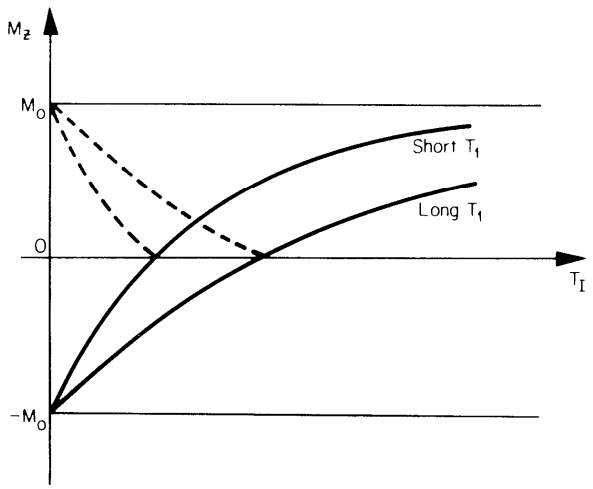


FIG. 2. Relaxation of longitudinal magnetization ($M_z$) after 180° inversion rf pulses. The initial negative magnetizations (solid lines) are inverted to positive values (dotted lines) by taking magnitude.

## NEW PROPOSED PHASE-CORRECTION SCHEME FOR THE REAL CONTRAST VALUE REPRESENTATION OF IR IMAGE

To avoid the polarity reversal in the IR images and eliminate phase errors, $\beta$ and $\alpha$ given in Eq. [6] should be either evaluated or measured. In the proposed new scheme, $\beta$ and $\alpha$ are measured and calculated from experimental data obtained from the conventional saturation–recovery (SR) pulse sequence using the spin-echo technique and are used for the IR imaging. Although some flow effects are expected, it is assumed in this paper that either the flow components are relatively small compared with stationary components or flow velocity is negligibly small.

*Evaluation of $\beta$ and $\alpha$*

At first, $\beta$ is measured in the saturation–recovery mode with $g_y = 0$ (where the echo signal is at maximum in the $y$ direction) in reference to the ideal echo time ($t_x = 0$), i.e., $\beta$ is estimated by the following relation:

$$|\hat{S}_s(t_x, 0)| \leq |\hat{S}_s(\beta, 0)| = |S_s(0, 0)| \qquad \text{for all } t_x, \qquad [8]$$

where $\hat{S}_s(t_x, t_y)$ and $S_s(t_x, t_y)$ are the phase-error corrupted and ideal echo signals obtained by SR sequence, respectively, and the equality is valid when $t_x = \beta$. It should now be observed that $\hat{S}_s(t_x, t_y)$ and $S_s(t_x, t_y)$ are equal to $\hat{S}_I(t_x, t_y)$ and $S_I(t_x, t_y)$, respectively, except that $\rho_I(x, y)$ is replaced by $\rho_s(x, y)$ which is given as

$$\rho_s(x, y) = \rho(x, y)\exp\left(-\frac{T_E + t_x}{T_2}\right)\cdot\left\{1 - 2\exp\left(-\frac{T_R - T_E/2}{T_1}\right) + \exp\left(-\frac{T_R}{T_1}\right)\right\}. \qquad [9]$$

From Eq. [9] it is easy to see that $\rho_s(x, y)$ is always positive and real at any echo time $T_E$ and repetition time $T_R$. Therefore, Eq. [8] is always valid since $\rho_s(x, y)$ which is the Fourier transform of $S_s(t_x, t_y)$ is a positive real value. In practice, additional care should be taken to confirm that the peak value $\hat{S}_s(\beta, 0)$ is correctly sampled so that estimation is exact. A useful way of avoiding errors in the $\beta$ measurement is oversampling in the echo signal domain. Another solution to sampling dependent error elimination is the use of some numerical data treatment techniques such as Lagrange interpolation (discussed in the Appendix).

Now, from the estimated $\beta$, $\alpha$ can be calculated by

$$\alpha = \tan^{-1}\left\{\frac{\mathrm{Im}[\hat{S}_s(\beta, 0)]}{\mathrm{Re}[\hat{S}_s(\beta, 0)]}\right\} \qquad [10]$$

where $\mathrm{Im}[\cdot]$ and $\mathrm{Re}[\cdot]$ are the $\beta$-phase-corrected imaginary and real parts of the echo signals, respectively.

These measured and calculated $\beta$ and $\alpha$ in the SR mode can now be used to calculate the $f_I(\omega_x, \omega_y)$. However, it is imperative to keep the measuring (SR mode) and IR imaging pulse sequences as similar as possible, since the phase errors are sensitive to the effects of electronics such as gradient pulse shapes, eddy current effects, repetition time, etc. Fortunately IR and SR sequences are identical except that the IR sequence has an additional preceding 180° inversion rf pulse. The measurement of $\beta$ and $\alpha$, therefore, can be achieved by simply using SR with sufficiently long repetition time $T_R$ and eliminating the 180° inversion rf pulse in the beginning of the IR imaging

sequence. This is illustrated in the pulse sequence shown in Fig. 3. Although this pulse sequence can be used at every $g_y$ encoding step, it usually suffices to take only the first pulse sequence and then the measured and calculated values of $\beta$ and $\alpha$ can be used for the rest of IR imaging pulse sequences.

## EXPERIMENTAL RESULTS AND DISCUSSIONS

For the demonstration of the new phase-corrected inversion–recovery (IR) imaging sequence, human brain imaging was carried out with the 1.5-kG KAIS NMR imaging system and the results are shown in Fig. 4. Figures 4a, c and e on the left side are the images obtained using existing IR imaging techniques (method employing the magnitude technique, see Eqs. [4] and [7]) while the images on the right side (b, d and f) are the ones obtained by the new phase-correction method. (a) and (b), (c) and (d), and (e) and (f) are the images obtained at different inversion times, i.e., (a) and (b) at $T_I$ = 150 ms, (c) and (d) at $T_I$ = 300 ms, and (e) and (f) at $T_I$ = 450 ms. As expected, with short inversion time, i.e., $T_I$ = 150 ms, most parts of the image are contrast reversed with respect to the phase-corrected image (compare the images shown in Figs. 4a and b). At $T_I$ = 300 ms, this contrast polarity reversal appears less prominent due to the fact that most spins are positive (see Fig. 2) and begin to show more consistent image contrasts from this time region. Further increase of $T_I$ up to $T_I$ = 450 ms clearly shows positiveness of the spins in most regions except the very long $T_I$ regions. Further quantitative study of the data obtained from phantom imaging is given in Fig. 5. The phantom is composed of $MnCl_2$ solution in various concentrations. In Fig. 5, curves

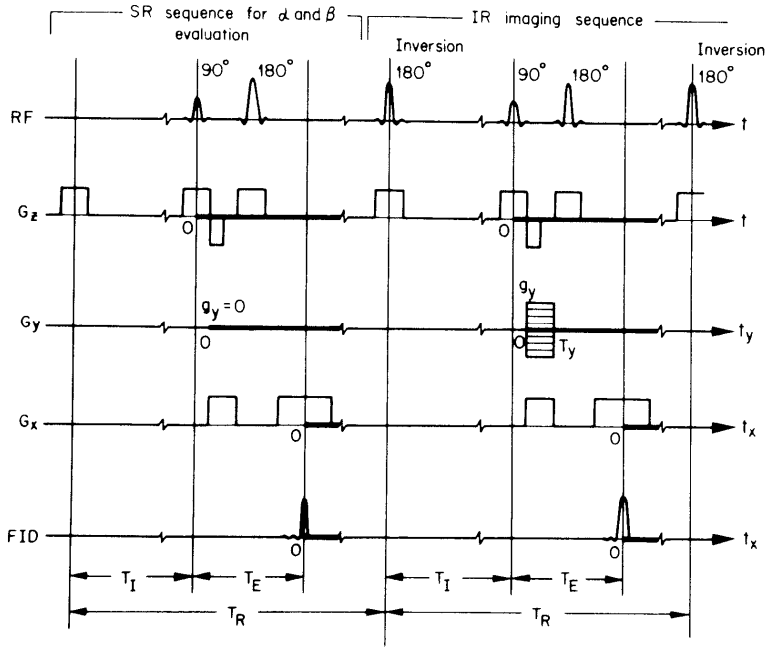


FIG. 3. Pulse sequence for new proposed IR imaging using the phase-correction method.

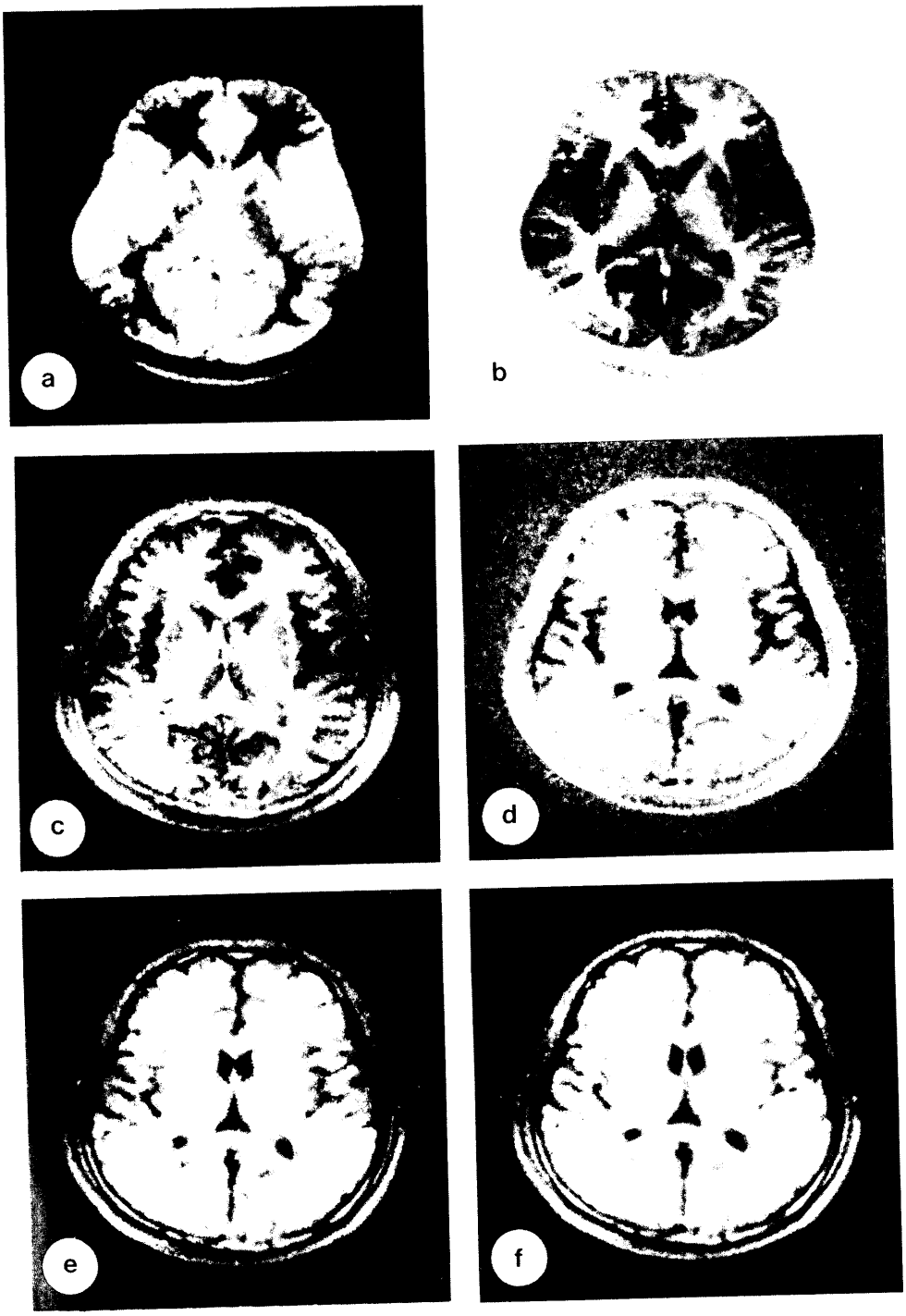


FIG. 4. Normal human head images with 1.5-kG KAIS NMR imaging system. Images (a), (c), and (e) are obtained by the magnitude method, while (b), (d), and (f) are obtained by the proposed phase-correction method. Repetition and echo times employed are $T_R$ = 1300 ms and $T_E$ = 30 ms, respectively. Inversion times of $T_I$ = 150 ms for (a) and (b), $T_I$ = 300 ms for (c) and (d), and $T_I$ = 450 ms for (e) and (f) are used for this experiment.

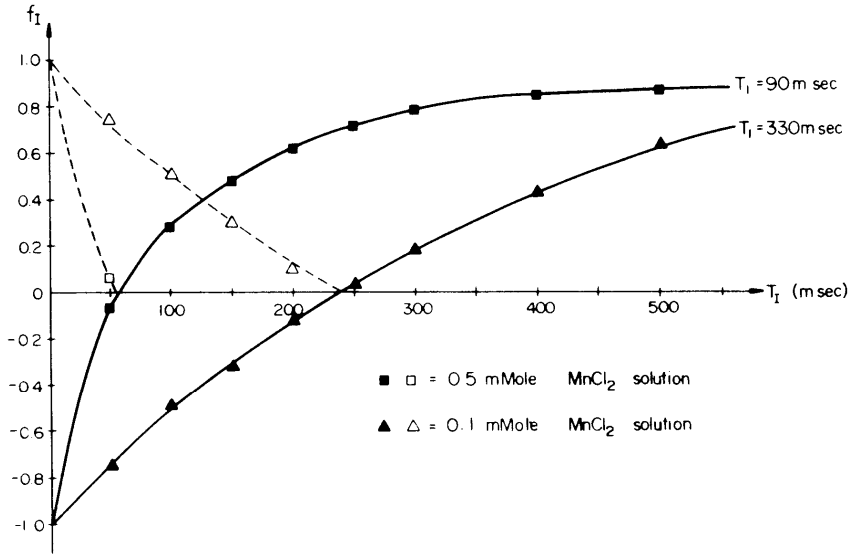


FIG. 5. Extracted values of the $f_I$ (normalized $\rho_I$) from the phantom images at several different inversion times $T_I$. Each point is the average value from a region of interest. Dotted lines and solid lines represent the values taken from magnitude method and phase-correction method, respectively. $T_R$ = 1300 ms and $T_E$ = 300 ms are used.

shown with dots are the values taken with the magnitude technique, while solid lines are the ones with the proposed new technique. It is thus proved that the use of new phase-corrected IR imaging shows consistent image contrasts and eliminates contrast reversal at shorter $T_1$ ranges ($\simeq$100–300 ms, e.g., for human brain imaging at 1.5-kG field strength). As mentioned earlier, consistent contrast images obtained at several different inversion times $T_1$ are found to be clinically important and this new phase-correction method would be of value.

## APPENDIX: ACCURATE ESTIMATION OF PHASES $\beta$ AND $\alpha$ IN THE SAMPLED ECHO SIGNAL

In the process of estimation using the echo signal obtained by Eq. [8], it is important to oversample the data sufficiently so that estimation of the peak, i.e., $\beta$, is accurate under the given sampling condition. It is often difficult to provide sufficiently oversampled echo data due to the limitations of the electronic parts such as the analog-to-digital converter. Another alternative, as suggested earlier, is use of accurate interpolation techniques and estimation of the peak value thereafter. In the present experimental condition, we found it useful to employ a simple Lagrange interpolation technique to be described in the following.

Exact echo center point $\beta$ is obtained from the sampled echo signal by the use of five point Lagrange interpolation as follows:

$$|\tilde{S}_s(t_x, 0)| = \sum_{k=\beta'-2}^{\beta'+2} |\tilde{S}_s(k\Delta t, 0)| P_k \qquad \text{[A-1]}$$

where $\beta'$ is the echo center point measured from the sampled echo signal by Eq. [8], $\Delta t$ is the sampling time interval of the analog-to-digital converter, and $P_k$ is the Lagrange polynomial given as

$$P_k = \prod_{\substack{j=-2 \\ j\neq k-\beta'}}^{2} \frac{t_x - (\beta' + j)\Delta t}{\{k - (\beta' + j)\}\Delta t}. \qquad \text{[A-2]}$$

From Eq. [A-1], a maximum value $\tilde{S}_s(\beta, 0)$ can be estimated by

$$\frac{\partial}{\partial t_x} |\tilde{S}_s(t_x, 0)| = 0 \qquad \text{[A-3]}$$

with a restriction

$$\left| \frac{t_x}{\Delta t} - \beta' \right| < 1. \qquad \text{[A-4]}$$

The solution of Eq. [A-3] is calculated using Bairstow's method given in Ref. (*14*). The unique solution $t_x$ which is calculated from Eqs. [A-3] and [A-4] is related to exact echo point $\beta$ as $\beta = t_x$. Estimation of $\beta$ by this method under critically sampled conditions is found to be useful for the phase-corrected inversion–recovery imaging discussed in this paper.

Using estimated $\beta$ from Eqs. [A-3] and [A-4], the center value of echo signal, $\tilde{S}_s(\beta, 0)$, is calculated by Lagrange interpolation given in Eq. [A-1]. Phase $\alpha$ can then be estimated more accurately from the interpolated $\tilde{S}_s(\beta, 0)$ and Eq. [10].

## REFERENCES


1. P. C. LAUTERBUR, *Nature (London)* **242,** 190 (1973).
2. Z. H. CHO, H. S. KIM, H. B. SONG, AND J. CUMMING, *Proc. IEEE* **70,** 1152 (1982).
3. W. S. HINSHAW, *J. Appl. Phys.* **47,** 3709 (1976).
4. G. JOHNSON, J. HUTCHISON, AND L. EASTWOOD, *J. Phys. E* **15,** 74 (1982).
5. A. KUMAR, E. WELTI, AND E. ERNST, *J. Magn. Reson.* **18,** 69 (1975).
6. P. MANSFIELD AND P. MORRIS, "NMR Imaging in Biomedicine," Academic Press, New York/London, 1982.
7. W. A. EDELSTEIN, P. A. BOTTOMLEY, H. R. HART, AND L. S. SMITH, *J. Comput. Assist. Tomogr.* **7,** 391 (1983).
8. I. R. YOUNG *et al., J. Comput. Assist. Tomogr.* **6,** 1 (1982).
9. F. W. WEHRLI *et al., J. Comput. Assist. Tomogr.* **8,** 369 (1984).
10. C. BAKKER, C. DE GRAAF, AND P. VAN DIJK, *IEEE Trans. Med. Imaging* **MI-3,** 197 (1984).
11. T. NEWTON AND D. POTTS (Eds.), "Advanced Imaging Technique," Chapter 3, Clavadel Press, 1983.
12. C. H. OH, H. S. KIM, H. W. PARK, W. S. KIM, S. W. LEE, AND Z. H. CHO, *IEEE Trans. Nucl. Sci.* **NS-30,** 1899 (1983).
13. C. H. OH, H. W. PARK, AND Z. H. CHO, *IEEE Trans. Med. Imaging* **MI-3,** 170 (1984).
14. S. S. KUO, "Computer Applications of Numerical Methods," Addison–Wesley, Reading, Mass., 1972.